

International Conference on Space Optics—ICSO 2018

Chania, Greece

9–12 October 2018

Edited by Zoran Sodnik, Nikos Karafolas, and Bruno Cugny



Space validation of 1550nm DFB laser diode module

Philip Henderson

Adrian Norman

John MacDougall

Paul Naylor

et al.



Space Validation of 1550nm DFB Laser Diode Module

Philip Henderson^a, Adrian Norman^a, John MacDougall^a, Paul Naylor^a, Efstratios Kehayas^{*a},
Lip Sun How^b, Sébastien Lhuillier^b, Alain Bensoussan^c, Mustapha Zahir^d

^aGooch & Housego, Broomhill Way, Torquay, TQ2 7QL, UK;

^bAdvEOTec, 6 Rue Closerie, ZAC Clos Pois, 91090 Lisses, France;

^cThales Alenia Space, 26 Avenue Jean François Champollion, 31100 Toulouse, France;

^dESA - ESTEC, Keplerlaan 1, PO Box 299, NL-2200 AG Noordwijk, The Netherlands

*ekhayas@goochandhousego.com; phone 44 1803 611743; fax 44 1803 611702; www.goochandhousego.com

ABSTRACT

Following a program funded by the European Space Agency, a novel laser-diode module has been created and tested to ESCC-23201-compliant space standards. Manufactured by Gooch & Housego, the module is set for imminent entry to the European space market for use in optical signal-processing and telecom systems. Emission is from a 1550nm DFB semiconductor laser diode driven at constant nominal current and temperature. Combined with a wavelength stability of better than $\pm 0.1\text{nm}$ and internal data rate of up to 3.2GHz, innovative sub-design and packaging provides for a unique power capability comprising a start-of-life ex-fibre power of $>90\text{mW}$ and a typical electric power consumption that, at $<4.1\text{W}$, is down to 25% of that of similar products. Validation testing by AdvEOTec (France) indicates a comprehensive set of space compliances such as in proton irradiation, humidity, hot/cold storage, rapid depressurisation, vibration and 1,000g shock, as well as immunity to $\pm 8\text{kV}$ of ESD, 10^{-5}mbar of vacuum, and 100krad of gamma irradiation. Unique methodologies for life-test modelling and production screening, established by Thales Alenia Space (France), provisionally confirm a 15-year space-compliant operating life. Space-compliant product, as presented, is intended to be supplied for a period of at least 5 years.

Keywords: Space validation, distributed feedback (DFB), laser diode

1. INTRODUCTION

As an established component in terrestrial signal-processing and telecom systems, the 1550nm DFB laser is potentially a key enabling technology in low-Earth-orbit (LEO) downlinks, inter-satellite relays, LEO constellations, and photonic telecom payloads. Previous development by Gooch & Housego [1] has reached the finished module shown in Figure 1.

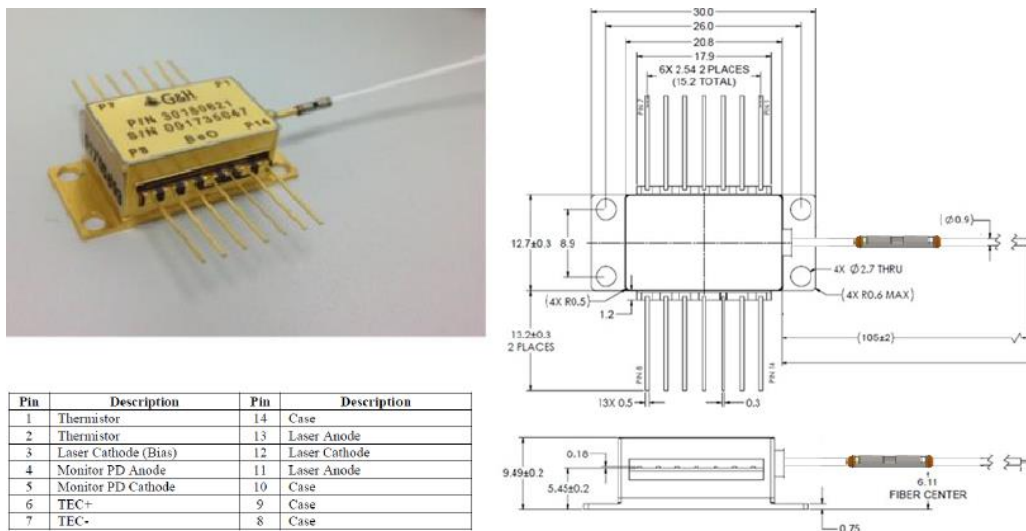


Figure 1. Finished laser module.

Such modules have a DFB laser diode emitting at 1550nm, a thermo-electric cooler (TEC) for maintaining the laser diode at constant temperature, a 14-pin butterfly-housing, full hermeticity attained via laser-welding technology, and a polarisation-maintaining fibre pigtail. Combined with a constant (derated) laser-drive specification of 375mA, the modules also offer 32dB of optical isolation and 3.2GHz of 3dB-bandwidth for high-speed direct data modulation.

In this paper, we report on the completion of pre-test module characterisation, the conduct of a full program of ESCC-23201-compliant [2] space validation, and the meticulous evaluation of device screening and reliability analysis that would indicate suitability for space-qualified operation.

2. PRE-TEST FUNCTIONAL PERFORMANCE

Following pre-cap inspection, fine and gross leak testing, and PIND, an investigation of functional performance yielded the key data shown in Figure 2.

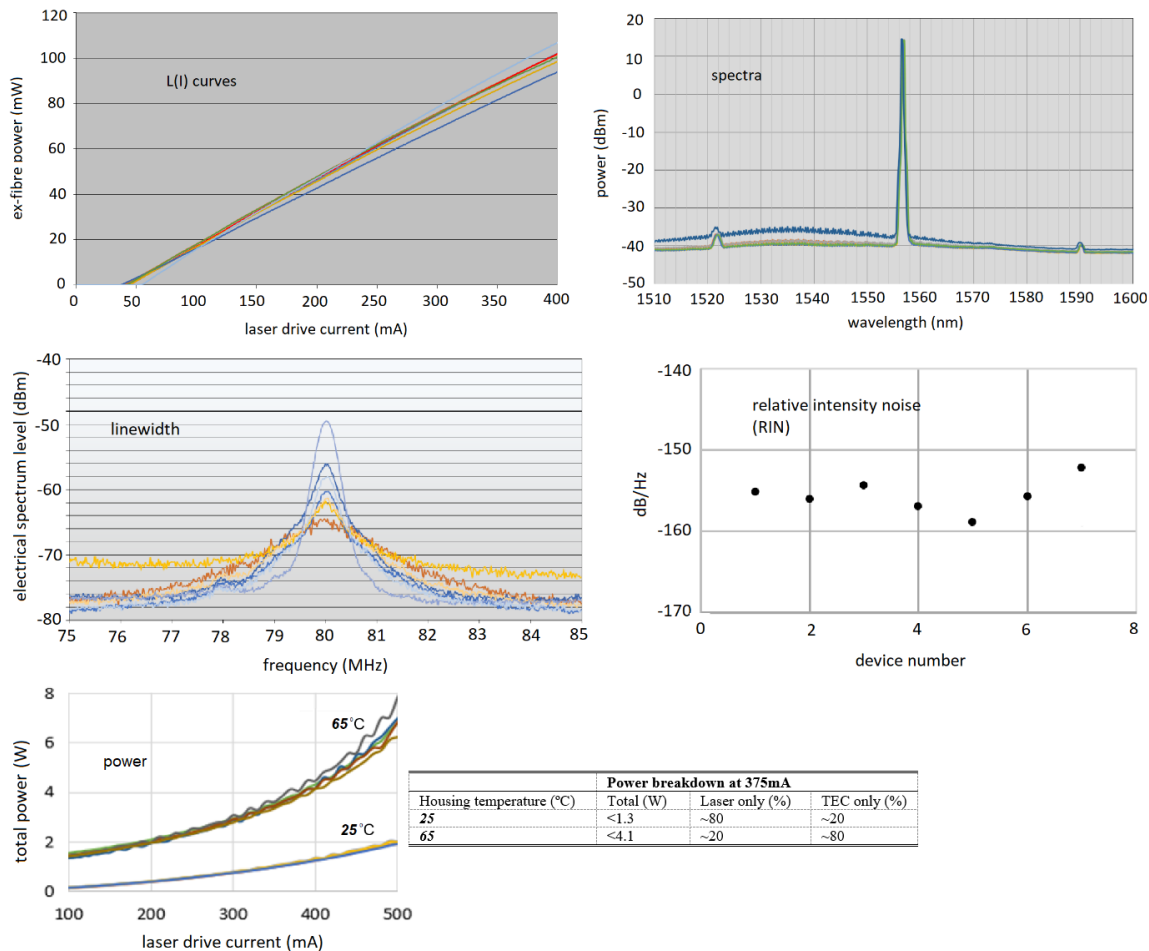


Figure 2. $L(I)$ curves, spectra, linewidth, RIN values, and electrical power consumption at typical extreme housing temperatures, as assessed over 7 random pre-test modules.

The $L(I)$ curves at 375mA indicate an ex-fibre power of >90mW, while the spectra confirm a side-mode-suppression ratio of >50dB. The linewidth measurements follow the methodology of the delayed self-homodyne interferometer which shifts the resultant spectra to the 80MHz range and wherein the optical linewidth is half that of the electrical linewidth. The laser linewidth is thus confirmed as between 200kHz and 1000kHz. For RIN, all measurements are less than -150dB/Hz. For electric power, total consumption is <4.1W at 375mA laser-drive current and 65°C housing temperature. Such a notably low consumption is attributed to the internal sub-assembly arrangement, which optimises the temperature control efficiency. It is further evident that at 25°C housing temperature, the power consumption is dominated by the laser, and the TEC contribution dominates only at much higher housing temperatures. Table 1 summarises the performance data.

Table 1. Pre-test functional performance.

Parameter	Agreed Detail Specification	Pre-test measurements
Laser drive current (mA)	375 (constant, derated value)	375 (by derated specification)
Laser temperature (°C)	25 (constant, typical value, controlled by TEC)	25 (typical specification)
Housing temperature (°C)	-20 minimum, +65 maximum	25 and 65 where indicated
Ex-fibre power (mW)	>56 (start of life)	>90
Side mode suppression ratio (dB)	>50	>50
Relative intensity noise (dB/Hz)	<-140	<-140
Linewidth (kHz)	<1000	<1000
Power consumption @ 25°C housing (W)	<8	<1.3
Power consumption @ 65°C housing (W)	<8	<4.1

The pre-test functional data are thus in comfortable compliance with the agreed Detail Specification.

3. VALIDATION PERFORMANCE

By following the ESCC-23201 evaluation test program for laser diodes [2], the scope of the validation is as defined in Figure 3, covering 57 unscreened modules. This number is slightly lower than in [2] as, for each subgroup, the number of parts is optimised for relevancy of results.

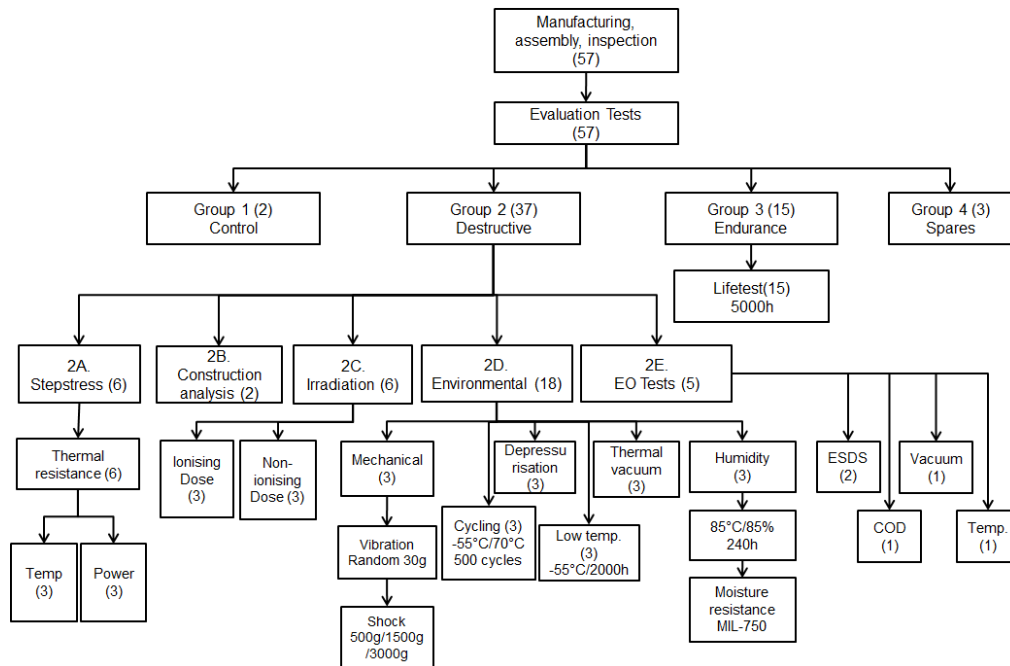


Figure 3. The validation-testing program (wherein: (xx) is the number of tested modules, EO = electrooptical, ESDS = electrostatic discharge sensitivity, Temp = temperature, COD = catastrophic optical discharge).

3.1 Evaluation plan methodology

With the lot of 57 laser modules considered as a representative manufacturing population, the evaluation started with an initial characterisation encompassing $L(I)$, $V(I)$, spectrum, low level $I(V)$, relative intensity noise (RIN) and linewidth. The laser diodes were accordingly found to have nominal ex-fibre powers between 70 and 100mW, and threshold currents between 35mA and 65mA. Then, under evaluation testing, measurements were repeated at each test step, allowing any slight variation in the laser parameters to be determined. To allow assessment of the reliability of the technology, the Figure 3 test groups encompass step-stressing, environmental testing, irradiation, electro-optic capability and endurance.

3.2 Step-stress sub-group

This concerned an evaluation of the effects of step-stressing of laser temperature between -25°C and 50°C, and output power above 100mW (with the laser current ranging from 450mA to 525mA). No major defect was noted and no significant drift was observed on the laser performance. Figure 4 illustrates the monitoring of output power drift with time.

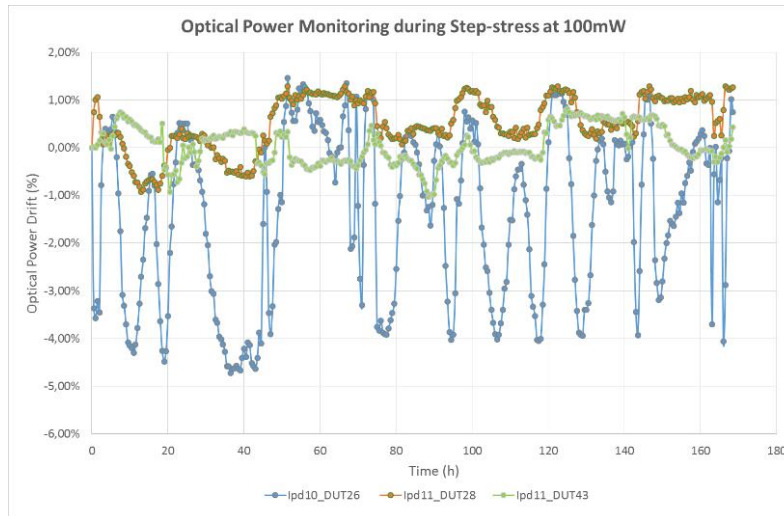


Figure 4. Power monitoring during the test at 100mW.

3.3 Environmental sub-group

Mechanical testing concerned 30g rms random vibration followed by half-sine shocks from 500g/1ms up to 1500g/0.5ms; Figure 5a shows samples subjected to random vibration. Temperature cycling concerned 500 rapid thermal cycles between -55°C and 70°C with an average ramp of 15 deg/min and dwell time of 15 minutes. Depressurisation involved rapid pressure cycling down to 10mbar over 5 seconds at ambient temperature, and with the laser diodes driven at 375mA and 30°C. Low temperature testing concerned 2000h of non-biased storage at -55°C. Thermal vacuum testing comprised 1000h of secondary vacuum at $<10^{-5}$ mbar with the laser diodes driven at 375mA and 30°C, and the module case temperature held at 65°C. Humidity testing concerned 240h of 85°C/85% damp heat, followed by -10°C to +50°C temperature cycling around the dew point.

For all the environmental tests, the modules showed no significant drifts except for the shock test where the limit is 1000g/0.5ms, and rapid thermal cycling wherein one of three laser diodes failed, indicating sensitivity of the module to fast temperature variation. The latter sensitivity is to be screened as discussed in Section 4.

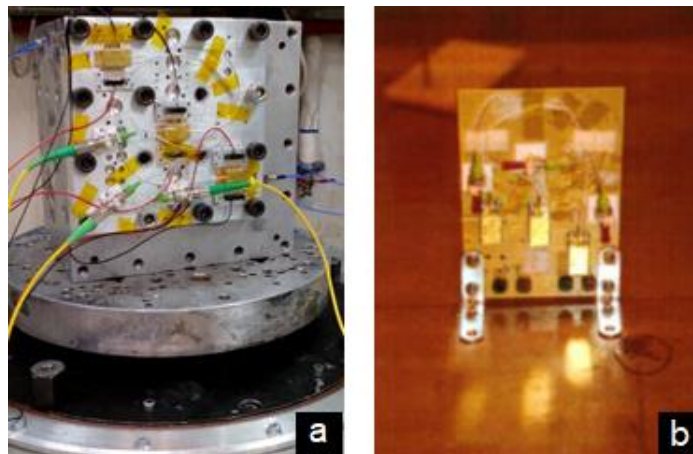


Figure 5. (a) Laser modules on mechanical shaker, and (b) devices inside the gamma radiation chamber.

3.4 Irradiation sub-group

Under radiation testing, both ionising dose and non-ionising dose were considered. The ionising dose was provided by gamma irradiation (total dose of 100 krad), whereas the non-ionising dose was provided by proton irradiation (total fluence of 10^{12} p+/cm² for an energy of 30 MeV). After both gamma and proton irradiation, no significant drift was observed on the laser diode. As expected, only the monitoring photodiode drifted after proton exposure. Figure 5b shows the samples inside the gamma radiation chamber.

3.5 Electro-optic sub-group

In this group, 4 types of tests were concerned. First, characterisation was conducted at extreme temperatures of -20°C and $+65^{\circ}\text{C}$. No major issues were encountered. Second, characterisation was conducted under secondary vacuum (around 10^{-5}mbar) under various temperatures of laser-diode and module-case. Relative to similar measurements in air, no differences were noted. The spectra given in Figure 6 illustrate the effect of different temperatures of laser-diode and module-case.

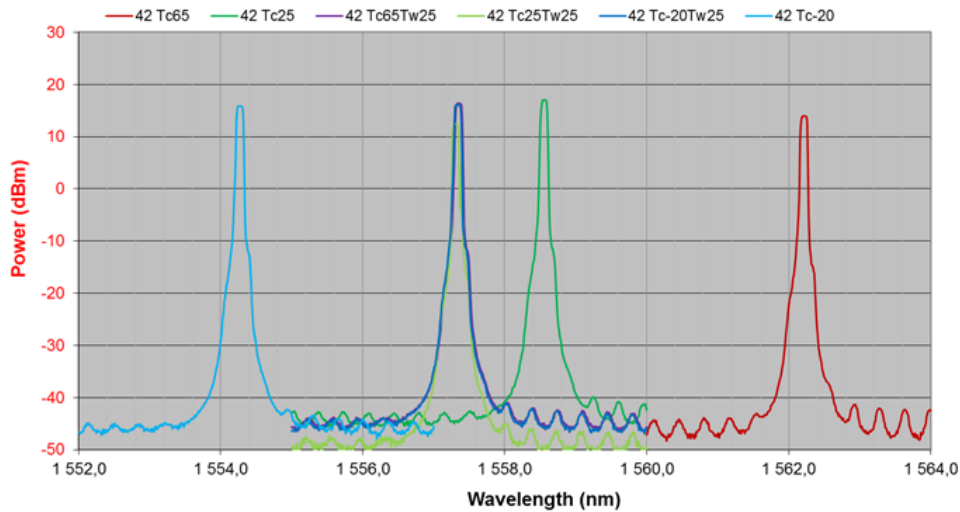


Figure 6. Optical spectrum at various module-case and laser-diode temperatures, Tc and Tw.

Third, electro-static discharge sensitivity was evaluated following the Human Body Model (HBM) of MIL-STD-883 standard, method 3015 [3]. As per Figure 7, the tested laser modules showed no degradation up to the 8kV step.

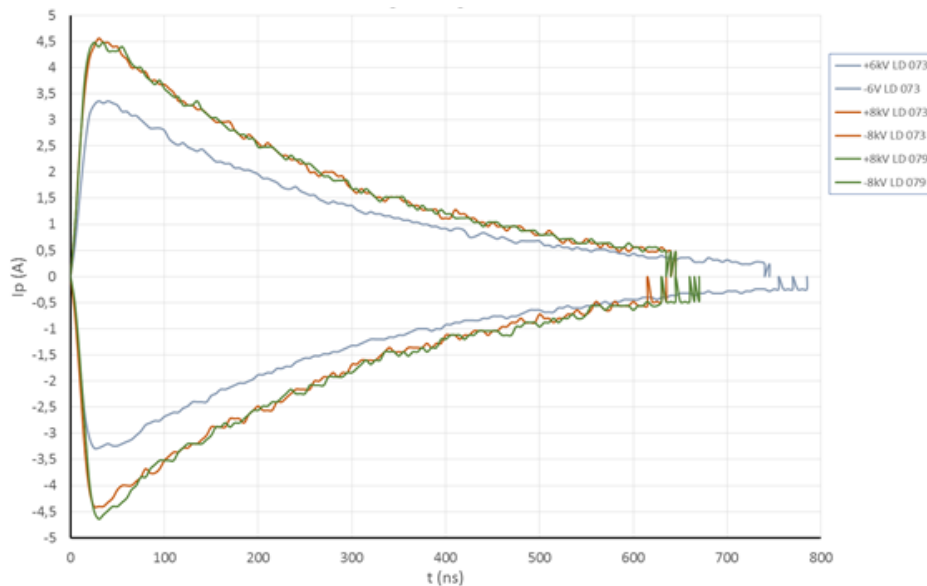


Figure 7. Pulse monitoring during the test at +/-6kV and +/-8kV on laser modules.

Fourth, catastrophic optical damage (COD) was investigated wherein the laser current is increased until failure and the forward voltage, optical power and laser temperature were continuously monitored. The resultant $L(I)$ curves are shown in Figure 8. We note the typical $L(I)$ bell shape in which the optical signal extinguishes after a laser current of 1A and is reversible thereafter; this shows that the laser diode can be driven up to 1.8A without degradation and verifies its robustness to high electrical current.

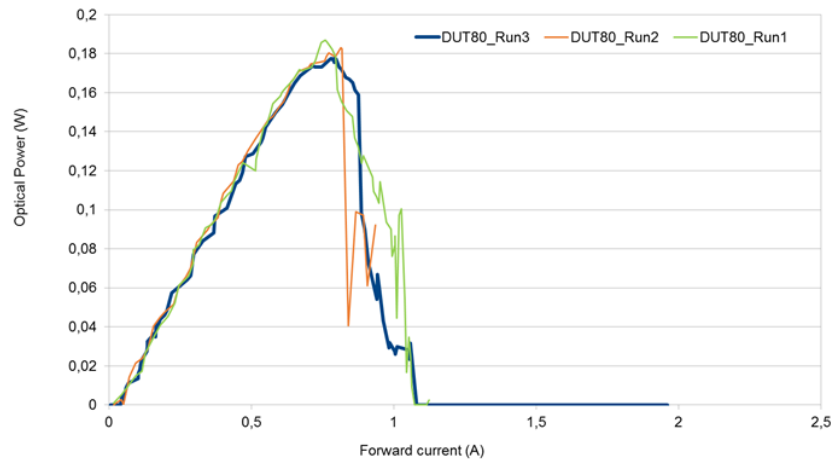


Figure 8. $L(I)$ curves obtained over 3 COD test runs.

3.6 Endurance sub-group

Life-testing was performed on 15 laser modules at a case temperature of 65°C for 5000h. The laser diode was driven at a current of 375mA and a temperature of 30°C. The in-situ monitoring of the optical power is represented by Figure 9.

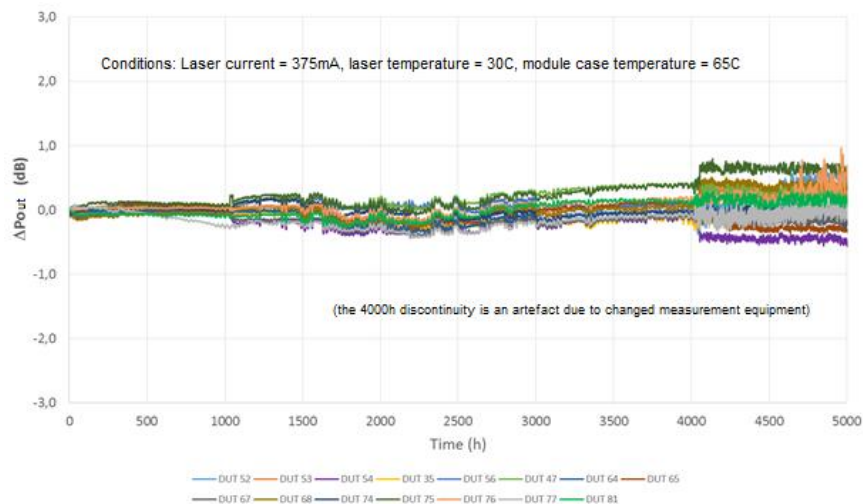


Figure 9. $L(I)$ Optical power drift ΔP_{out} during life-testing.

The stability of the laser diodes illustrated by Figure 9 indicates minimal drift over the 5000h life-test.

3.7 Evaluation test conclusion

With optical output power exceeding 70mW, no catastrophic failures were encountered, and the samples were shown to be robust to thermo-mechanical as well as to radiation tests. With potential space compliance summarised as in Table 2, two significant points concern the mechanical shock level which is limited to 1000g/0.5ms, and the coupling sensitivity to rapid temperature change. Near-term addressing of the latter point is by screening, as discussed in Section 4.

Table 2. A summary of ESCC-23201 [2] based evaluation.

Strength	Weakness
Robust to ESD until $\pm 8kV$	Optical alignment sensitive to rapid thermal cycling ($-55^{\circ}C/70^{\circ}C$ $15^{\circ}C/min$)
Robust to COD until 1.8A	Module can withstand mechanical shocks up to 1000g
Robust to Irradiation up to 100krad and $10^{12}p+/cm^2$	Internal monitoring photodiode very sensitive to ESD and irradiation
Robust to vacuum to 10^{-6} mbar	Tricky thermal management
Robust to 5000h of Life Test at $65^{\circ}C/375mA$	

4. PERFORMANCE ANALYSIS AND RELIABILITY PREDICTION

4.1 Introduction

For validation-tested devices to be assured of fulfilling mission profiles, their random failure rate must be below the maximum accepted rate, and their Mean-Time-To-Failure (MTTF) for parametric wear-out must be greater than the mission lifetime. Figure 6 is a schematic of the bathtub curve and the conditions to be fulfilled.

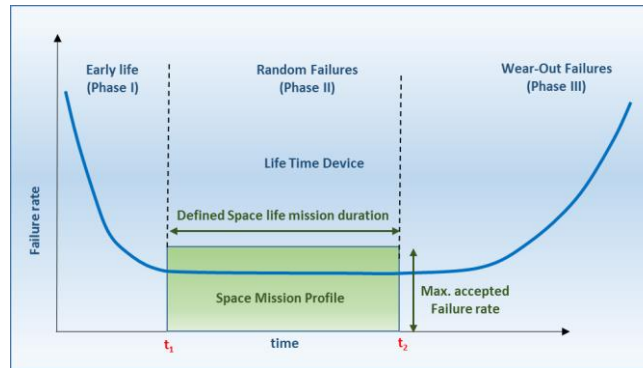


Figure 6. Bathtub curve and Satellite mission profile limits.

According to the Telcordia quality standard [4], the time to failure τ for laser diodes follows two types of models:

- for random failures, τ_{random} is considered as the Arrhenius temperature law:

$$\tau_{random}(T_{wave}, I_{nom}, V_{nom}) = \tau_0 \cdot \exp\left(\frac{E_{a_random}}{k \cdot (T_{wave} + R_{th} \cdot I_{nom} \cdot V_{nom} - P_{out}(I_{nom}))}\right) \quad (1a)$$

- and, for wear-out failures, $\tau_{wearout}$ is considered as the Eyring law:

$$\tau_{wearout}(T_{wave}, I_{nom}, V_{nom}) = \tau_1 \cdot \left(\frac{I_{nom}}{I_{burnout}}\right)^{-2} \cdot \exp\left(\frac{E_{a_wearout}}{k \cdot (T_{wave} + R_{th} \cdot I_{nom} \cdot V_{nom} - P_{out}(I_{nom}))}\right) \quad (1b)$$

where τ_0 is a constant, E_{a_random} (the activation energy for random failure) = 0.35eV, k (Boltzmann's constant) = 8.617×10^{-5} eV/K, T_{wave} is the temperature of the laser diode chip (as set by the TEC), R_{th} (the thermal resistance of the laser diode) is evaluated by a non-destructive method to be in the range [8.8 K/W, 10.4 K/W], I_{nom} and V_{nom} are the nominal laser current and voltage biasing conditions, P_{out} is the nominal optical output power, $I_{burnout}$ is the laser current that leads to instantaneous catastrophic failure, and $E_{a_wearout}$ (the activation energy for wear-out failure) = 0.4eV. In particular, we can note that by removing the operational bias factor $(I_{nom}/I_{burnout})^{-2}$ from Equation 1b, $\tau_{wearout}$ becomes consistent with an Arrhenius (pure thermal) law.

However, our module's components are carefully selected, characterised, and assembled according to space-quality standards (in particular ECSS-Q-ST-60-05 [5]) and do not exhibit random failure. Hence only Equation-1b wear-out applies. Also, with spectral stability ensured through operating the laser diode at constant current and temperature, and with change in dynamic line-width (or frequency chirp) having already demonstrated strong technological stability, our work highlights ex-fibre power P_{out} is the only affected parameter. This is seen to be, to a very limited extent, during life-testing of the laser diode. Such degradation differs from that in other electronic devices due to the recombination of electron-hole pairs and the presence of high optical densities within the active region and at the output facet [6]. The applicable degradation mechanisms are (i) defect formation in the active region, and (ii) degradation of current-confining junctions [7]. As first observed in AlGaAs lasers and LEDs, the defect structures generally comprise dark spot defects (DSDs) and the dark line defects (DLDs) of the (100) crystal direction. Operation at high injected current densities creates high-energy electrons and holes, thermal gradients, potential for strain fields, and a high non-radiative recombination rate inside the active region. This, in turn, can promote the motion, multiplication, and growth of isolated defects into clusters. Although InGaAsP/InP buried double heterostructure laser diodes are less vulnerable to some of the dominant degradations mechanisms of other technologies (e.g. GaAs, InGaAs, InP, etc) [8], [9], the fact remains that reliability can still be critical according to the specific epitaxial growth, blocking layers, and (in DFB lasers) the selectivity of the engraving of the Bragg grating. In particular, in empiric studies on the technology by Fukuda *et al.* [10], it was found that activation energies for generating DSDs and DLDs are respectively 0.16eV and 0.2eV, that the generation time of the first DSD depends strongly

on the operating current density, and that the time to failure follows the factor $\exp(A \cdot J^2)$, where A is a constant and J is the current density.

Since, in addition to temperature, degradation is enhanced by increasing the laser current and output power, aging studies are conducted in one of the following two modes of operation. The first is constant current aging – often referred to as ACC mode (automatic current control) – where the laser current is held constant for the duration of the test. The second is constant power aging, which is often referred to as APC mode (automatic power control). Under APC, the optical output power is measured either with an external photodetector or by using an internal monitor photodiode if one is available within the laser package, and this power is then held constant by continuously adjusting the laser current as required to maintain constant output power. While constant power aging is frequently used as a mimic of typical operation, our work uses constant current because this mode is essential to achieving the specified operating-wavelength of within $\pm 0.1\text{nm}$.

In practice, difficulties in laser diode life testing arise from temperature instability, equipment measurement and control instability, equipment reliability, and power failures. A challenge associated with temperature control is the self-heating of the laser during operation. The temperature elevation at junction level is in the range [8K, 10K] at the maximum rated bias current of 375mA (and bias voltage of 2.4V). Additionally, heat-sink temperature fluctuations as small as 0.1°C manifest as noise in the measurement of optical power due to the temperature sensitivity of laser output power at a given current. Finally, if an external photodetector is used to measure optical output power, its temperature must also be controlled to ensure stable measurements. Laser diode life test studies require an accurate measurement of changes in laser operating parameters as small as a few percent over thousands of hours. Consequently, the stability of the measurement equipment must be on the order of 0.1% per 1000 hours. In most locations, occasional electrical power failures are inevitable during the course of a multi-thousand-hour life-test study. In many cases, it is impractical to provide battery backup systems due to the high power required for heating in life test systems. As a result, the life test system must handle power failures without damage to the lasers, and must be able to resume a test precisely after power is restored.

To model the resultant changes in ex-fibre power P_{out} , we follow [11] wherein the Eyring law of Equation 1b is extended via the so-called Boltzmann-Arrhenius-Zhurkov (BAZ) model. Hence, the time to failure τ for the combined action of an elevated temperature T and external stress represents S is written as in Equation 1c.

$$\tau = \tau_A \cdot \exp\left(\frac{E_a - \gamma \cdot S}{k \cdot T}\right) \quad (1c)$$

where S is can be any stimulus or group of stimuli (such a voltage, current, signal input, irradiation, etc), τ_A is a pre-factor, γ is a factor of loading characterising the role of the level of stress, and the product $\gamma \cdot S$ is the stress per unit volume and is measured in the same units as the activation energy E_a . By considering multiple stresses including temperature, the approach offers the establishment of a unified reliability model for electronic devices operating under multiple-stress harsh environments; whether submarine, nuclear, on the ground, in transport, or in aerospace.

The changes in ex-fibre power P_{out} , which are also seen under temperature cycling, can be mitigated by screening. According to the Telcordia standard [12], laser modules should normally be 100% screened according to:

- 20 temperature cycling between the limits of -40°C and $+70^\circ\text{C}$ for CO applications and -40°C and $+85^\circ\text{C}$ (or between minimum and maximum storage temperatures) for RT/Unc applications; the associated pass/fail criteria are {a} a 5% or greater change in front-to-back tracking ratio and/or coupling efficiency, and {b} no obvious change (beyond measurement error) in threshold current.
- 96 hours of APC burn-in at 70°C for CO or 85°C for RT/UNC ambient temperature, and maximum-rated optical output power; and the associated failure criterion is a 5% or greater increase in threshold or drive current.

In terms of production burn-in screening, the challenge is to achieve high manufacturing throughput and accurate measurements at very low cost. The two most common strategies are the following:

- Burn-in with in-situ measurement: In the case of low production volumes, or when the same system is used for both engineering evaluations and burn-in, it is often cost effective to perform parametric measurement in the same system. In this case, data may be taken continuously or at the beginning and end of a burn-in cycle.
- Burn-in with separate measurement: In almost all other cases, it is more cost effective to use simple constant current, constant temperature burn-in chambers which are separate from the parametric test system. A semi-automated measurement system can easily provide the throughput required to process over 1,000 lasers in an eight-hour shift. This approach also has the advantage that the measurement test system can also be designed to incorporate spectral measurement which is difficult to implement in an in-situ system.

4.2 Application and results

With regard to Equation 1b, we consider that the expression suffers a lack of precision at the limit when the current flow is zero since the implied infinite time to failure at $I_{nom}=0$ is inconsistent with the Arrhenius law limit. To overcome this contradiction, we propose to update the Eyring model as in Equation 1d.

$$\tau_{wearout}(T_{wave}, I_{nom}, V_{nom}) = \tau_1 \cdot \left(\frac{I_{burnout} - I_{nom}}{I_{burnout}} \right)^n \cdot \exp\left(\frac{E_{a_wearout}}{k \cdot (T_{wave} + R_{th} \cdot I_{nom} \cdot V_{nom} - P_{out}(I_{nom}))} \right) \quad (1d)$$

where, by using the ratio $(I_{burnout} - I_{nom})/I_{burnout}$ instead of $I_{nom}/I_{burnout}$, a value of 1 is obtained at $I_{nom}=0$ which makes $\tau_{wearout}$ consistent with the Arrhenius (pure thermal) law of Equation 1a. The power factor n is then calculated by equivalence to Equation 2b, with the result obtained given in Equation 1e.

$$n = 3.8 \quad (1e)$$

A life-test sequence was performed on 15 DFB laser modules at case temperature, $T_{case} = 65^\circ\text{C}$, for 5000 hours. Also, the laser current I_{nom} and laser temperature T_{wave} were set at constant respective values of 375mA and 30°C . We measured the devices at interim times during this ACC stress. A linear drift of output power from 1000 to 5000h was observed with a maximum value close to 4%. Based on a median ranking parameter and the time to failure t_i for a part i , linearly extrapolated to reach the 30% drift, a Weibull plot was obtained as shown in Figure 7.

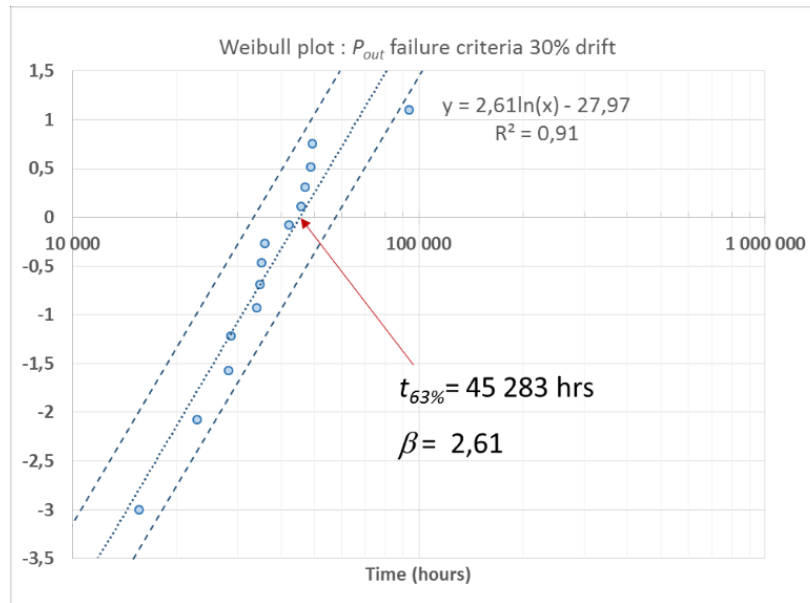


Figure 7. Weibull plot considering $\Delta P_{out}=-30\%$, $I_{nom}=375\text{mA}$, $T_{wave}=30^\circ\text{C}$ and $T_{case}=65^\circ\text{C}$; the dashed line shows 95% CL.

The analysis shows the lot of devices to be homogeneous, and extracts a Weibull β parameter of $\beta=2.61$. Extracted data for a range of ΔP_{out} values are in Table 3.

Table 3. Extracted reliability data using $I_{nom}=375\text{mA}$, $T_{wave}=30^\circ\text{C}$ and $T_{case}=65^\circ\text{C}$ for various values of ΔP_{out} .

ΔP_{out} failure criterion (%)	Weibull β parameter	Mean time to failure (MTTF) (yr)	Failure rate (FIT)
-10	3.70	2	4758
-30	2.61	5	1782
-50	2.43	9	1096

Other values of predicted MTTF and $\tau_{wearout}$ may be obtained through changed values of current (I_{nom}) and temperature (T_{wave}) applied to the laser diode. First, Equation 1c may be simplified by noting that the temperature of the junction T_j of the laser diode is given by Equation 2.

$$T_j = k \cdot (T_{wave} + R_{th} \cdot I_{nom} \cdot V_{nom} - P_{out}(I_{nom})) \quad (2)$$

Then, considering user and test-stress levels of laser current and junction temperature (respectively I_{user} , I_{stress} , T_{j_user} and T_{j_stress}), we may deduce an accelerating factor AF from Equations 1c, 1d and 2 as given in Equation 3:

$$AF = \frac{\tau_{wearout}(I_{nom}=I_{user}, T_j=T_{j_user})}{\tau_{wearout}(I_{nom}=I_{stress}, T_j=T_{j_stress})} = \left(\frac{I_{burnout}-I_{user}}{I_{burnout}-I_{stress}} \right)^{3.8} \cdot \exp\left(\frac{E_a}{k} \cdot \left(\frac{1}{T_{j_user}} - \frac{1}{T_{j_stress}} \right) \right). \quad (3)$$

With $E_a=0.4\text{eV}$ as manufacturer data, and user values reduced to $I_{user}=275\text{mA}$ and $T_{wave_user}=20^\circ\text{C}$, we may then deduce AF as 3.27 and update the Table-3 data as in Table 4.

Table 4. Updated MTTF and failure rate data considering $I_{nom}=275\text{mA}$ and $T_{wave}=20^\circ\text{C}$.

ΔP_{out} failure criterion (%)	Mean time to failure (MTTF) (yr)	Failure rate (FIT)
-10	6	1333
-30	17	499
-50	28	307

Accordingly, we demonstrate an MTTF of >15 years under $I_{nom}=275\text{mA}$ and $T_{wave}=20^\circ\text{C}$ operating conditions, taking $\Delta P_{out}=-30\%$ as an acceptable failure criterion.

Nevertheless, these preliminary data are a first assessment of MTTF and FIT values, and need to be consolidated with additional steady-state life-testing as follows:

- 2 to 3 junction temperatures (e.g. using $T_{wave}= 50^\circ\text{C}$, 80°C and 100°C) to confirm the $E_a=0.4\text{eV}$ manufacturer data.
- 3 laser biasing conditions (e.g. $I_{nom}=350\text{mA}$, 375mA and 400mA) to confirm Equation-1's $n=3.8$ power factor.

To quantify the degradation of the laser diode with junction temperature T_j , we empirically define the laser threshold current I_{th} and the external differential quantum efficiency η_D as in Equation 4.

$$I_{th} = I_0 \cdot e^{\frac{T_j}{T_0}}, \text{ and } \eta_D = \eta_0 \cdot e^{-\frac{T_j}{T_1}} \quad (4)$$

where $T_0=198\text{K}$, $T_1=178\text{K}$, $I_0=10.2\text{mA}$ and $\eta_0=1.32\text{W/A}$.

To permit quantification of all potential manufacturing, testing and operational failures of the module's laser diode (whether arising from electrical biasing, atmospheric, radiation-based, thermo-mechanical, or other applied environmental stresses), we implement the BAZ-modelling approach by setting $x\%=I_{nom}/I_{burnout}$ within Equation 1d, and then using Equation 2 to give:

$$\tau_{wearout} = \tau_0 \cdot \exp\left\{ \left(\frac{E_{awearout}}{k \cdot T_j} \right) \cdot \left[1 + \frac{n \cdot k \cdot T_j \cdot \ln(1-x\%)}{E_{awearout}} \right] \right\}. \quad (5)$$

We now set

$$\gamma_I = \frac{n \cdot k \cdot T_j}{E_{awearout}} \quad (6)$$

to obtain

$$E_{a_eff}(x\%) = E_{awearout} \cdot [1 + \gamma_I \cdot \ln(1 - x\%)]. \quad (7)$$

It is thus seen that the effective activation energy depends on stress condition applied, and varies linearly with the current bias applied as a first approximation. As a numerical example, we can assess $\gamma_I = 0.246$ and $E_{a_eff} = 0.347\text{eV}$ based on the following typical data: $T_{wave}=20^\circ\text{C}$, $I_{nom}=375\text{mA}$ (=75% of the maximum 500mA rating), $I_{th}=50\text{mA}$, $V_{nom}=2.4\text{V}$, $n=3.8$, $E_a=0.4\text{eV}$, $R_{th}=9.6\text{K/W}$, $P_{out}=80\text{mW}$, and $I_{burnout}=900\text{mA}$. Figure 8 represents the effective activation energy E_{a_eff} as function of the stress condition ($x\%=I_{nom}/I_{burnout}$) applied. Accordingly, E_{a_eff} decreases with $x\%=I_{nom}/I_{burnout}$.

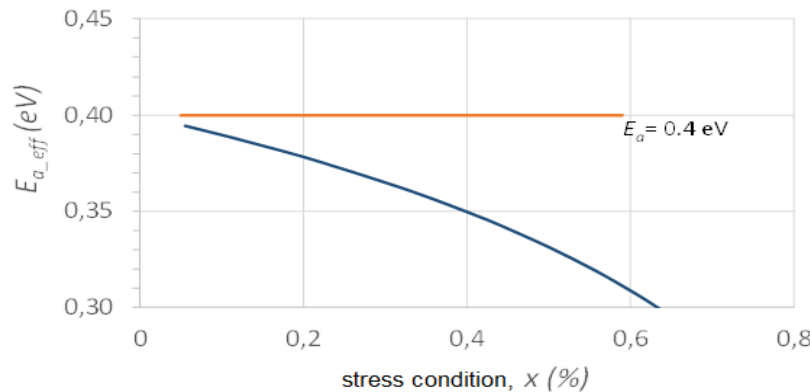


Figure 8. Effective activation energy E_{a_eff} versus applied current stress condition $x(\%)$ calculated for $T_{wave}=20^\circ\text{C}$.

4.3 Optimising the testing methodology for new laser-diode technology

Following Section 4.2, we recommend optimising the BAZ-model as per the following steps:

Step 1: Characterise the laser-diode lot in chip form, and at module level after screening, comprising:

- $L(I)$ plots with I ranging up to 75% of maximum rating, and for T_j ranging from 10°C to 90°C (each 20°C).
- $I(V)$ forward plots, in semi-log form, from 10nA to the maximum 500mA rating at 3 junction temperatures.
- $I(V)$ reverse plots with voltages ranging from -2V to 0V (at $T_j=20^\circ\text{C}$).
- Gauss distribution plots (complete lot) for main parameters (at $T_j=20^\circ\text{C}$, and over frequency range) comprising I_{th} , η_D , central wavelength characteristics, and RIN @375mA.
- Burnout failure conditions assessment (5 devices at initial) for high current drive limit at chip and module level (at $T_j=20^\circ\text{C}$) and related output power degradation or/and black line failure (increase of the drift of optical power).
- Leakage current ($I(V)$ plot in log-log scale at low injection current).

Step 2: Perform step-stressing according to Table 5, where 15 test devices and 2 extra control devices (CD) are suggested.

Table 5. Proposed modification to the step-stress testing of reference [2], including an update to the number of devices.

Parameter	Original implementation	Proposed implementation (+2 CD)	
Thermal resistance	AdvEOTec procedure	6/6 AdvEOTec procedure	15/15
High temperature step stress	168h steps at: 50, and 55°C	2/6 48h steps @ 80, 90, and 100°C. Then 110°C continued to 4 failures. Bias setting at maximum laser current rating.	5/15
Low temperature step stress	168h steps at: -15, -20, and -25°C	1/6 48h steps @ -30, -40, and -50°C. Bias setting at maximum laser current rating.	5/15
Power step stress	168h steps at: 100, 105mW, and 115mW	3/6 48h steps @ 80, 90, and 100. Then 110mW continued to 4 failures. TEC adjusted at $T_j=40^\circ\text{C}$ for all steps.	5/15

Step 3: As consolidated from step-stress data to achieve more than 50% failure in a short period of time (typically close to 1000h), define an accelerated endurance program. Each test sequence is to include at least 6 devices, and involve 3 T_{wave} temperatures and 3 I_{nom} biasing conditions, that are proposed to be 50°C, 80°C, 100°C, 350mA, 375mA and 400mA. Perform testing and use control devices for every interim measurement. Use high temperature data to calculate E_a : this is the baseline of the BAZ model (use chip on carrier for simplification of measurement). Calculate values of n and γ .

Step 4: Repeat above methodology, where appropriate, for other stressing parameters – e.g. output power (may be done simultaneously as for current), and irradiation.

4.4 Key outcomes and proposals

Guaranteed reliability: Under, for example, at $I_{nom}=275\text{mA}$ and $T_{wave}=20^\circ\text{C}$, the analysis of Section 4.2 predicts <10% drift of lasing current threshold, <30% drift of output power, within $\pm 0.1\text{nm}$ drift of wavelength, and a 15yr MTTF.

Space-quality lot validation: For a 15-year operating life and an acceptable quality limit of 0.65%, we propose steady-state life-testing as in Table 6, and acceptable parametric drifts as in Table 7.

Table 6. Steady-state life-testing for lot validation.

Life-test characteristic	Symbol	Conditions	Units	Notes
Case temperature	T_{case}	65 (+0 -5)	°C	-
Chip temperature	T_{wave}	50	°C	Fixed by TEC
Current biasing	I	400	mA	ACC mode
Total duration	T	5000 (-0 + 24)	h	-
Number of devices	N	22	-	-
Measure as per Table 7	-	0, 240, 500, 1000, 1500, 2000, 3000, 4000, 5000	h	Sampling basis: 22 devices/0 defect

Table 7. Acceptable parametric drifts for lot validation.

Measurement characteristic	Symbol	Conditions	Min	Max	Units
Threshold drift	ΔI_{th}	-	-	20	%
Slope efficiency drift	$\Delta \eta_D$	$I=375\text{mA}$, $T_{wave}=20^\circ\text{C}$	-	20	%
Forward current drift	ΔI_{op}	$P_{op}=80\text{mW}$, $T_{wave}=20^\circ\text{C}$	-	20	%
Pout Kinfree drift	ΔI_K	-	-	20	%
Centre wavelength drift	$\Delta \lambda_0$	$I=375\text{mA}$, $T_{wave}=20^\circ\text{C}$	-50	50	pm
Spectral width drift	$\Delta(\Delta \lambda)$	$I=375\text{mA}$, $T_{wave}=20^\circ\text{C}$	-	20	%
Ex-fibre power drift	ΔP_{op}	$I=375\text{mA}$ and $P_{op}=50\text{mW}$, $T_{wave}=20^\circ\text{C}$	-	20	%

Screening and burn-in: Based on the obtained evaluation test data (Section 3), we recommend the following order of conditioning to be completed on a 100% basis for space lot delivery:

- 20 temperature cycles between the limits of -40°C and $+85^{\circ}\text{C}$; pass/fail criteria are {a} $\Delta P_{op} < 10\%$ at $I=375\text{mA}$ and $T_{wave}=20^{\circ}\text{C}$, {b} ΔI_{th} change in threshold current lower than 10%, and {c} current I_{op} required to maintain an optical output of $@P_{op}=50\text{mW}$ (at $T_{wave}=20^{\circ}\text{C}$) to have a change $<10\%$. Max number of failed devices is 5%.
- Burn-in as per Table 8: read and record P_{out} monitoring (ex-fibre) during stress sequence; the failure criteria are $>10\%$ increase (whichever occurs first) in {a} I_{th} threshold current @ $I_{op}=375\text{mA}$ and $T_{wave}=20^{\circ}\text{C}$, {b} slope efficiency η_D at the same conditions, and {c} drive current ΔI_{op} @ $P_{op}=50\text{mW}$ and $T_{wave}=20^{\circ}\text{C}$. Max number of failed devices is 5%.
- 100% hermeticity test (gross and fine leak). Max number of failed devices is 5%.
- Total lot Percentage Defective Allowed (PDA) not greater than 10% (all handling failures must be included).

Table 8. Burn-in conditions.

Characteristics	Symbol	Conditions	Units	Notes
Case temperature	T_{case}	50 (+0 -5)	$^{\circ}\text{C}$	-
Chip temperature	T_{wave}	35	$^{\circ}\text{C}$	Fixed by TEC
Current biasing	I	375	mA	ACC mode
Duration	t	168 (-0 + 24)	h	-
Measure as per lot validation (Table 7)	-	Pre and post burn-in	-	PDA after burn-in $<10\%$.

Maximum ratings: We propose these, from known device heritage and Section-3 data, as in Table 9.

Table 9. Absolute maximum ratings for some important parameters.

Parameter	Symbol	Maximum rating	Unit	Notes
Operating case temperature	T_{case}	-20 to +65	$^{\circ}\text{C}$	-
Storage temperature	T_{sto}	-40 to +85	$^{\circ}\text{C}$	-
Laser diode operating temperature	T_{wave}	30	$^{\circ}\text{C}$	Fixed by TEC
Laser diode forward current	I	500	mA	CW
Optical power in output fibre	P_{op}	130	mW	CW, at $I=500\text{mA}$

Operational ratings: Table 10 shows the main operational ratings for space applications, listed by key component.

Table 10. Some key operational ratings, where start-of-life and $T_{case} \in [0^{\circ}\text{C}, 50^{\circ}\text{C}]$ apply unless otherwise specified.

DC characteristics	Symbol	Test conditions	Min	Typical	Max	Units
Centre wavelength (quasi single mode, C-band)	λ_0	P_{op}	1530	(ITU grid)	1605	nm
LASER Laser chip set temperature for λ_0	T_{wave}	P_{op}	15	-	30	$^{\circ}\text{C}$
DIODE Spectral width CW mode FWHM	-	P_{op}	-	-	0.5	MHz
CW operating optical power in output fibre	P_{op}	$I=375\text{mA}$	65	-	-	mW
(TEC Slope efficiency	η_{slope}	$I=375\text{mA}$	0.35	-	0.4	mW/mA
current Conversion efficiency	η_D	$I=375\text{mA}$	20	-	35	%
adjusted Threshold current	I_{th}	-	20	-	90	mA
to obtain Wavelength drift with case temperature ($T_{wave}=20^{\circ}\text{C}$)-	-	$0^{\circ}\text{C} < T_{case} < 50^{\circ}\text{C}$	-	-	1	pm/ $^{\circ}\text{C}$
$T_{wave}(\lambda_0)$ Wavelength temperature tunability	-	$15^{\circ}\text{C} < T_{wave} < 30^{\circ}\text{C}$	0.08	-	0.12	nm/ $^{\circ}\text{C}$
Thermal resistance laser chip to cooler	R_{th}	$I=375\text{mA}, T_{wave}=20^{\circ}\text{C}$	-	-	10.5	K/W
TEC Cooling capacity	ΔTEC	$P_{op}, T_{case}=50^{\circ}\text{C}$	50	-	-	$^{\circ}\text{C}$
(1-stage element) Drive current	I_{TEC}	$\Delta\text{TEC}=50^{\circ}\text{C}, P_{op}, T_{case}=50^{\circ}\text{C}$	-	-	1.6	A
Drive Voltage	V_{TEC}	$\Delta\text{TEC}=50^{\circ}\text{C}, P_{op}, T_{case}=50^{\circ}\text{C}$	-	-	4.3	V
THERM- Resistance	$R_{thermistor}$	$T_{wave}=20^{\circ}\text{C}$	-	10	-	k Ω
ISTOR Constant	B	$T_{wave}=20^{\circ}\text{C}$	-	18.7	-	k Ω

Reliability testing methodology for new laser-diode technology: For this, we make the recommended optimisations as per Section 4.3.

5. TECHNOLOGICAL OUTLOOK

The validation-tested modules, as described, are intended to be supplied until at least 2023. Concurrent end-user investigations and in-flight mission demonstrations would assist the drive towards acceptance as a space-qualified product, suited to listing on the European Preferred Parts List. For the longer-term growth of global space initiatives, we anticipate a continuing program of supply that would feature an upgrading of design for improved specification and performance, reduced need for screening, and space-compatible delta qualification.

6. CONCLUSIONS

We have presented characterisation and space-validation results on a 1550nm DFB laser diode module manufactured by Gooch & Housego according to a program of work funded by the European Space Agency. In the near-term, excellent results are obtained in all critical areas that would allow space validation to be granted. Modules are available for immediate supply into global space markets.

ACKNOWLEDGEMENTS

This work has been supported by the European Space Agency through the ECI program "Space validation of DFB laser module at 1.55 μm " (ESA contract number 4000110310). We gratefully acknowledge ESA/ESTEC Technical Officer M. Zahir for his support and technical guidance during contract execution.

REFERENCES

- [1] MacDougall, J., Naylor, P., Elder, J., Henderson, P., Stampoulidis, L., Barbero, J., Kehayas, E., "Optoelectronic modules for space applications," Proc. SPIE 10562 (2017).
- [2] ESCC, [Evaluation test program guidelines for laser diode modules, ESCC basic specification 23201], ESA, Noordwijk, 1-22 (2014).
- [3] "Test Method Standard – Microcircuits," <http://www.landandmaritime.dla.mil/programs/milspec/ListDocs.aspx?BasicDoc=MIL-STD-883> (3 May 2018).
- [4] [Reliability prediction procedure for electronic equipment, SR-332], Ericsson (2016).
- [5] ECSS, [Space product assurance: Generic procurement requirements for hybrids, ECSS-Q-ST-60-05], ESA, Noordwijk, 1-77 (2009).
- [6] Mendizabal, L., [Thesis: Fiabilité des diodes laser DFB 1,55 μm pour des applications de télécommunication: Approche statistique et interaction composant-système], University of Bordeaux, Bordeaux (2006).
- [7] Agrawal, G. P., and Dutta, N. K., [Semiconductor lasers], Kluwer Academic Publishers, Norwell (1993).
- [8] Fukuda, M., [Reliability and degradation of semiconductor lasers and LEDs], Artech House, Boston & London (1991).
- [9] Mendizabal, L., Bechou, L., Deshayes, Y., Verdier, F., Danto, Y., Lafitte, D., Goudard, J., and Loué, F., "Study of influence of failure modes on lifetime distribution prediction of 1.55 μm DFB Laser diodes using weak drift of monitored parameters during ageing test," *Microelectronics Reliability Journal* 44(9-11), 1337-1342 (2004).
- [10] Fukuda, M., Wakita, K., Iwane, G., "Dark defects in InGaAsP/InP double heterostructure lasers under accelerated aging," *Journal of Applied Physics* 54, 1246 (1983).
- [11] Bensoussan A., Suhir, E., Henderson, P., and Zahir, M., "A unified multiple stress reliability model for microelectronic devices — Application to 1.55 μm DFB laser diode module for space validation," Proc. 26th European Symposium on Reliability of Electron Devices, 1729-1735 (2015).
- [12] [Reliability assurance for optoelectronic devices, GR-468-CORE], Ericsson (2004).